Electronic Supplementary Information

Core/shell Fe_3O_4/Gd_2O_3 nanocubes as T_1-T_2 dual modal MRI contrast agents

Fenfen Li,[a] Debo Zhi,[a] Yufeng Luo,[b] Jiqian Zhang,[c,d] Xiang Nan,[a] Yunjiao Zhang,[c] Wei Zhou,[c]

Bensheng Qiu,[a] Longping Wen,*[c] and Gaolin Liang*[b]*

[a]Center for Biomedical Engineering, Department of Electronic Science and Technology, University of Science and Technology of China, Hefei, Anhui 230027, China

[b]CAS Key Laboratory of Soft Matter Chemistry, Department of Chemistry, University of Science and Technology of China, Hefei, Anhui 230026, China

[c]School of Life Sciences, University of Science and Technology of China, Hefei, Anhui 230027, China

[d]Department of Anesthesiology, First Affiliated Hospital, Anhui Medical University, Hefei, Anhui, China

***Corresponding author:**

bqiu@ustc.edu.cn (B.-S. Q.), lpwen@ustc.edu.cn (L.-P. W.), gliang@ustc.edu.cn (G.-L. L.).

Contents:

Supporting scheme, figures, tables, references

Scheme S1. Illustration of the ligand exchange process. Oleic acid on the as-synthesized nanocubes was replaced by dopamine.

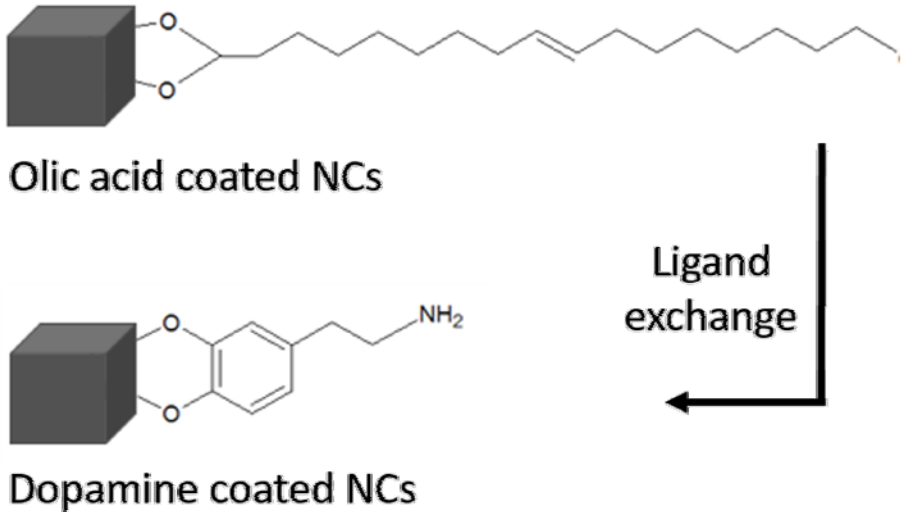

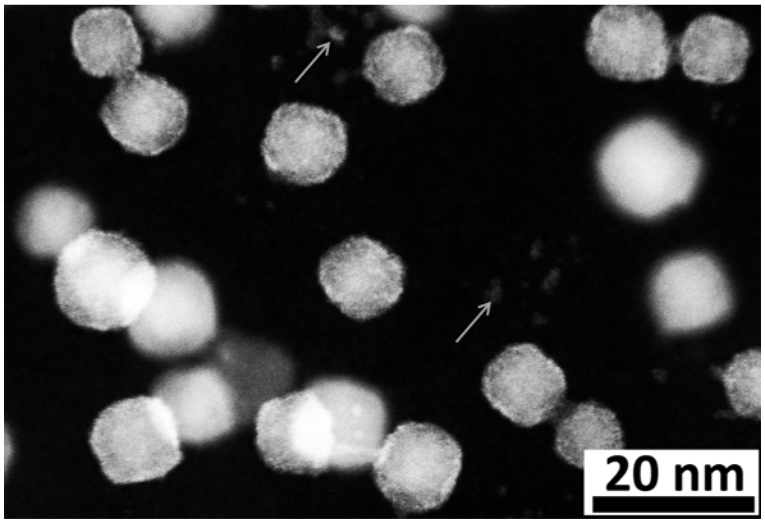

Figure S1. STEM-HAADF image of core/shell Fe_3O_4/Gd_2O_3 nanocubes. Withe arrows indicate the small nanocrystals.

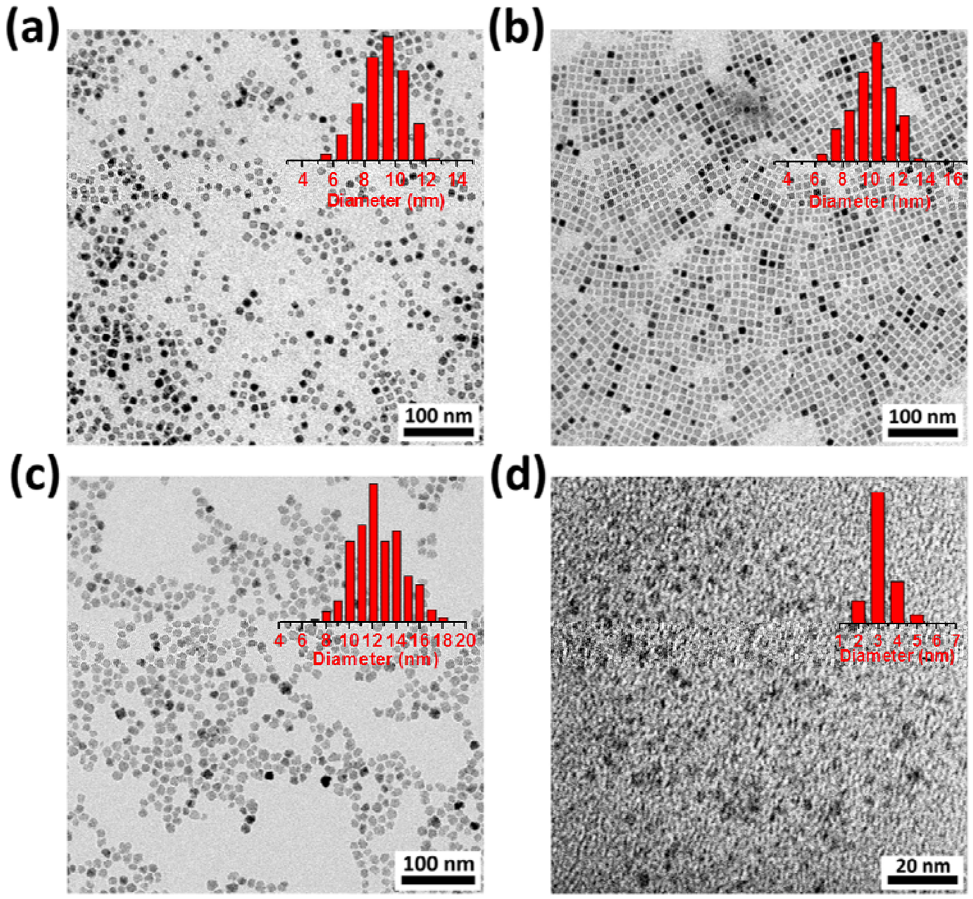

Figure S2. TEM images of (a) as-synthesized core/shell Fe_3O_4/Gd_2O_3 nanocubes, (b) as-synthesized Fe_3O_4 nanocubes, (c) the commercial water-soluable spherical iron oxide nanoparticles and (d) as-synthesized ultrasmall Gd_2O_3 nanoparticles. The insets are their size distribution analyses, which are 9.2 ± 1.4， 10.1 ± 1.6，11.8 ±2, and 2.7 ± 0.6 nm, respectively.

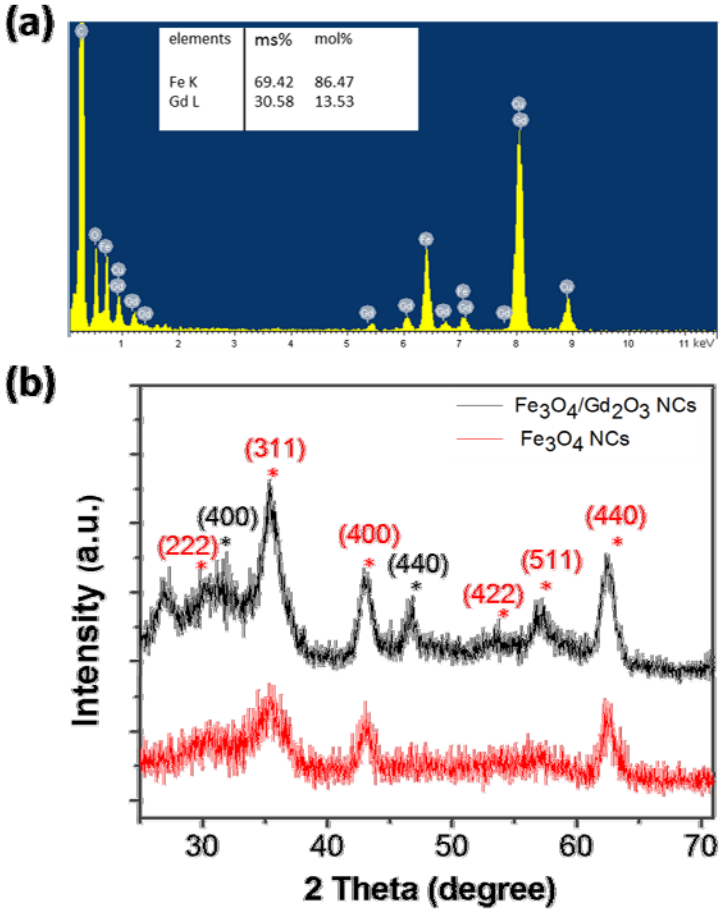

Figure S3. (a) The energy-dispersive X-ray spectroscopy (EDS) spectrum of as-prepared Fe_3O_4/Gd_2O_3 nanocubes. (b) XRD patterns of Fe_3O_4/Gd_2O_3 nanocubes (top) and Fe_3O_4 nanocubes (bottom). The diffraction peaks agree to the spinel structure of magnetite (red) and cubic Gd_2O_3 (black).

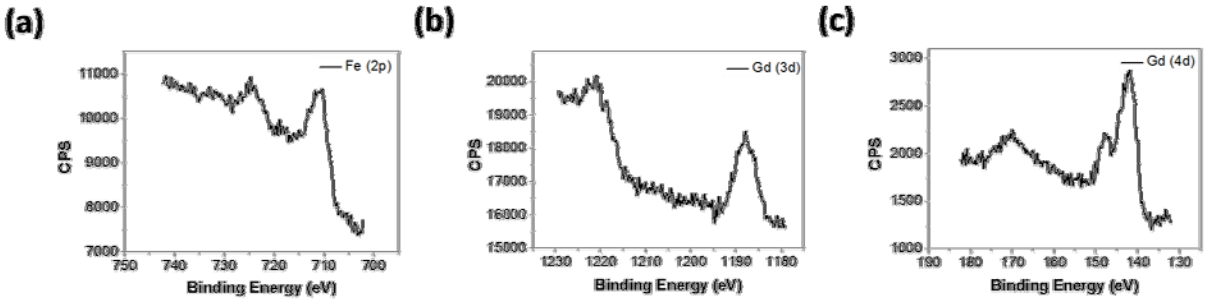

Figure S4. (a) XPS Fe 2p spectrum, (b) XPS Gd 3d spectrum, and (c) XPS Gd 4d spectrum of the Fe_3O_4/Gd_2O_3 nanocubes.

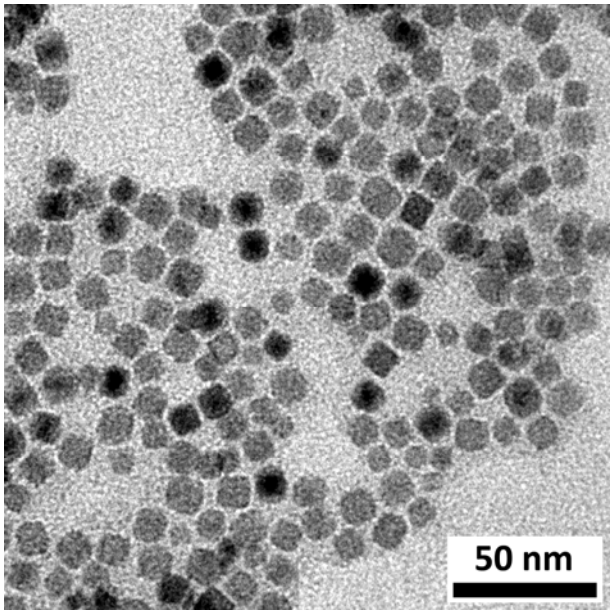

Figure S5. Water soluable dopamine-coated Fe_3O_4/Gd_2O_3 nanocubes.

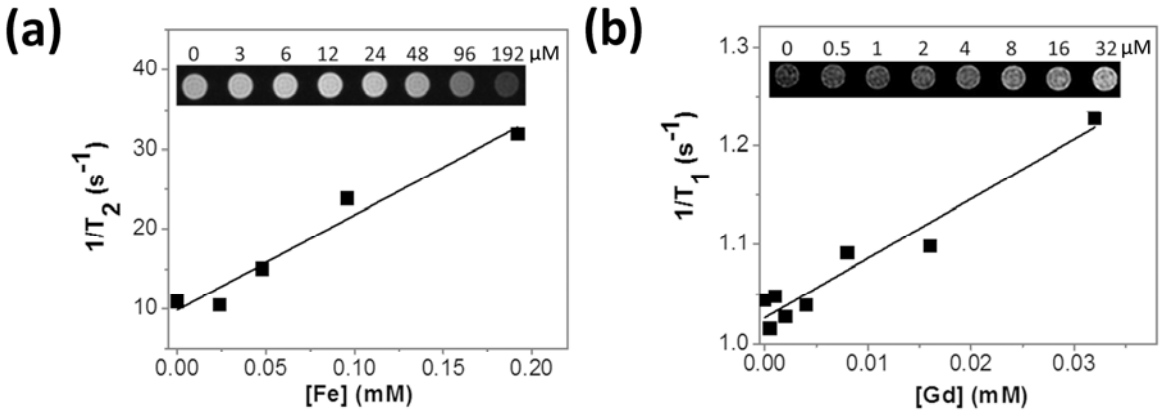

Figure S6. (a) Concentration-dependent transverse relaxation rate $1/T_2$ curves of spherical Fe_3O_4 nanoparticles over [Fe], which is 119.8 ± 14 $mM^{-1}s^{-1}$ (r_2). The inset is T_2-weighted MR images of Fe_3O_4 nanoparticles at different Fe concentrations. (b) Concentration-dependent longitudinal relaxation rate $1/T_1$ curves of Gd-DTPA over [Gd], which is 6.0 ± 0.6 $mM^{-1}s^{-1}$ (r_1). The inset is T_1-weighted MR images of Gd-DTPA at different Gd concentrations.

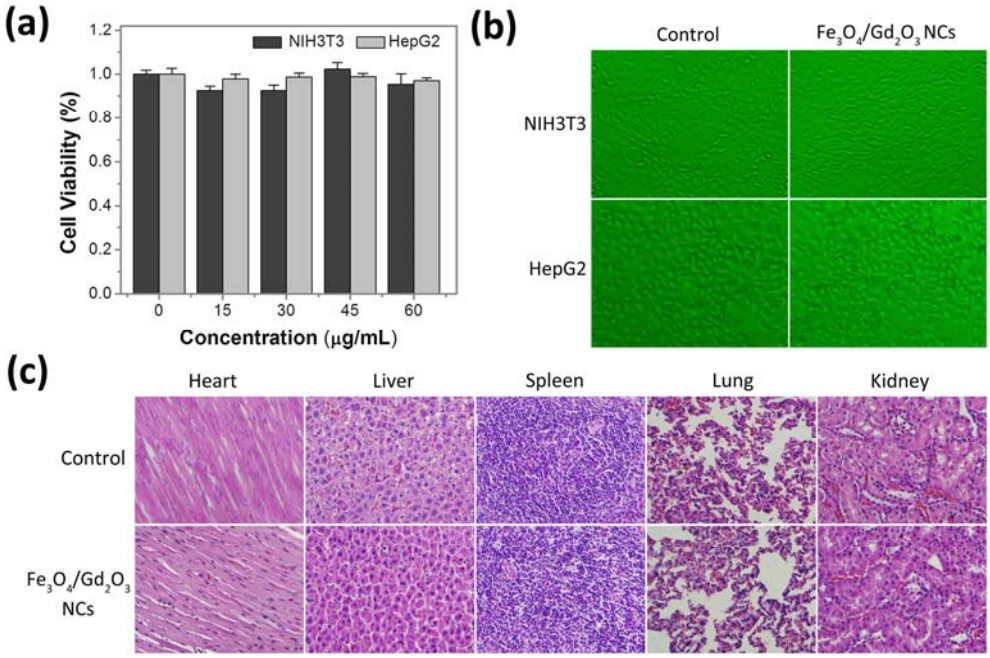

Figure S7. (a) MTT assay of NIH3T3 and HepG2 cells incubated with different concentrations of Fe_3O_4/Gd_2O_3 nanocubes for 24 h. (b) Cell morphology of NIH3T3 and HepG2 cells incubated with or without Fe_3O_4/Gd_2O_3 nanocubes at 60 μg Fe/mL for 24 h. (c) Heamatoxylin and eosin (H&E) of tissue sections from rats at 24 h post-injection with (bottom) or without (top) Fe_3O_4/Gd_2O_3 nanocubes, respectively.

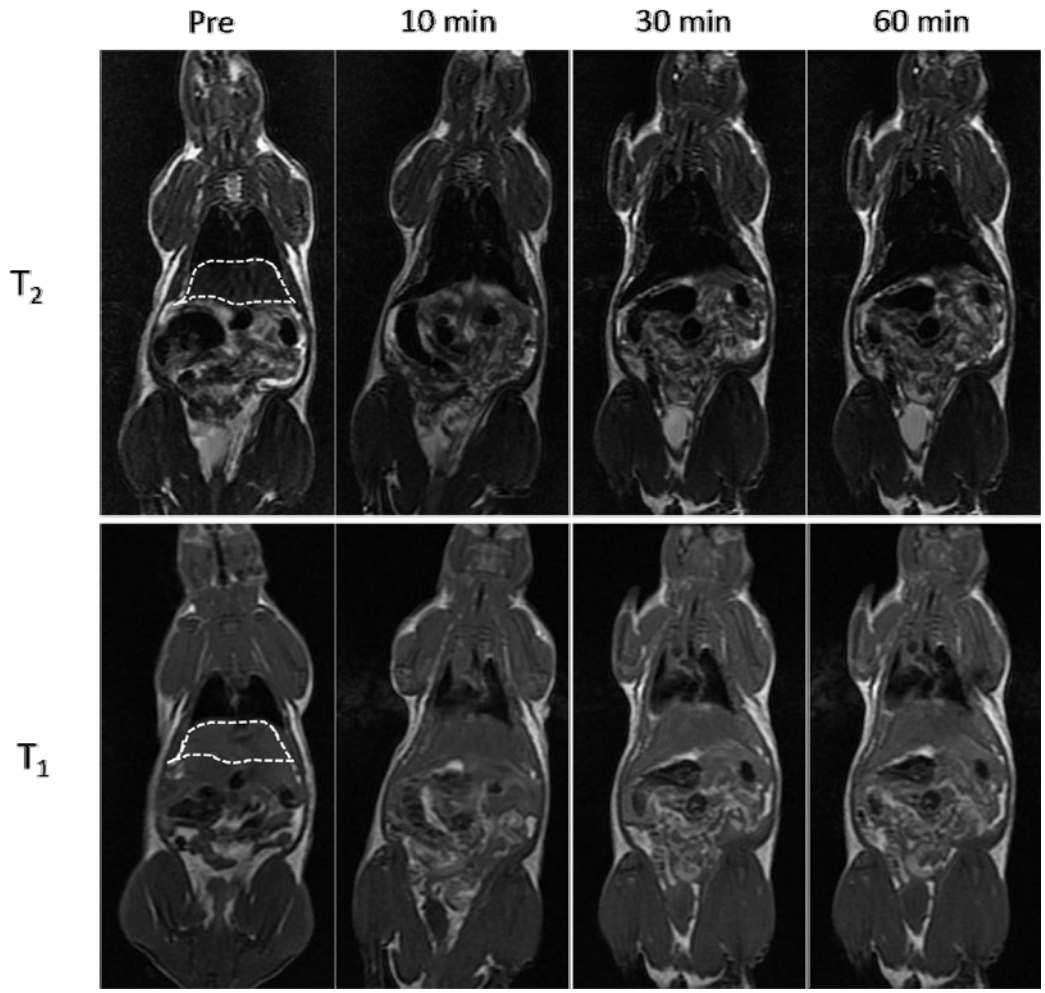

Figure S8. T_2- and T_1-weighted coronal MR images of rat at 3 T before and after intravenous injection of Fe_3O_4/Gd_2O_3 nanocubes at a dose of 2 mg Fe/kg.

Table S1. Comparison of transverse relaxation (r_2) of iron oxide nanoparticles with different morphologies.

NPs	Core size	Shape	Surface Coating	r_2 ($mM^{-1}s^{-1}$)	External field	Reference
Fe_3O_4	9.5	quasi-cubical	DMSA	61.3	1.5 T	1
Fe_3O_4	9.6	spherical	DMSA	52.7	1.5 T	1
[a]Fe_3O_4	30 (edge length)	octapod	HDA-G2	679.3	7 T	2
[a]Fe_3O_4	16	spherical	HDA-G2	125.86±9	7 T	2
[b]Fe_3O_4	20 (edge length)	octapod	HDA-G2	209.03±15	7 T	2
[b]Fe_3O_4	10	spherical	HDA-G2	59.91±6	7 T	2
Fe_3O_4	22 ± 2.6	cubic	PEG phospholipid	761	3 T	3
Fe_3O_4	23	spherical	OligoPEG-DOPA	254	11.7T	4

a (or b) samples are similar in geometric volume.

Table S2. MR signal-to-noise ratio (SNR) changes of liver pre- and post- injection of Fe_3O_4/Gd_2O_3 nanocubes at a dose of 2.0 mg/kg (n = 3).

	T_2 signal changes (%)			T_1 signal changes (%)		
	10 min	30 min	60 min	10 min	30 min	60 min
ΔSNR(axial)	36±2	51±3	49±5	6±2	10±2	7±1
ΔSNR (coronal)	58±4	64±1	62±8	4±3	14±5	8±3
Mean	47±3	58±2	56±6	5±2	12±3	8±2

Reference

1. M. Song, Y. Zhang, S. Hu, L. Song, J. Dong, Z. Chen and N. Gu, *Colloid. Surface.A*, 2012, **408**, 114-121.
2. Z. Zhao, Z. Zhou, J. Bao, Z. Wang, J. Hu, X. Chi, K. Ni, R. Wang, X. Chen, Z. Chen and J. Gao, *Nat. Commun.*, 2013, **4**, 2266.
3. N. Lee, Y. Choi, Y. Lee, M. Park, W. K. Moon, S. H. Choi and T. Hyeon, *Nano Lett.*, 2012, **12**, 3127-31.
4. H. B. Na, G. Palui, J. T. Rosenberg, X. Ji, S. C. Grant and H. Mattoussi, *ACS Nano*, 2012, **6**, 389-399.